

# 2D Magneto-Thermal Modeling of Coated High-Temperature Superconductors

François Roy<sup>\*1</sup>, Bertrand Dutoit<sup>1</sup>, Frédéric Sirois<sup>2</sup> and Francesco Grilli<sup>3</sup>

<sup>1</sup>F.Roy and B. Dutoit, EPFL, École Polytechnique fédérale de Lausanne

<sup>2</sup>F. Sirois, École polytechnique de Montréal

<sup>3</sup>F. Grilli, Los Alamos National Laboratory

\*Corresponding author: EPFL-IC-LANOS, Station 14, 1015 Lausanne, Switzerland [francois.roy@epfl.ch](mailto:francois.roy@epfl.ch)

**Abstract:** Thin films are very promising for the design of novel and efficient Fault Current Limiter (FCL) made of high-temperature superconductors (HTS). However, their thermal and highly non-linear electromagnetic behavior in the presence of over-critical currents is crucial to their use in future electrical grid. In this paper, we propose a numerical approach to solve magneto-thermal models for geometries of high aspect ratio. The used electromagnetic formulation, inspired in good part from the work of Brambilla et al. [1,2], were performed in 2D using *COMSOL Multiphysics*. Also, the thermal part of our model has been implemented to consider the thermal exchange with the nitrogen bath needed for HTS-FCL operation. Our simulations allow us to observe design limitations of FCL made of these new shaped conductors.

**Keywords:** Finite element methods, Fault current limiters, Thin film devices, High-temperature superconductors

## 1. Introduction

Recent advances in thin film technology and epitaxial growth allow the emergence of coated conductors (CC) as a second generation of high-temperature superconductors (HTS), which, by their expected low price and high critical current density, seems to be the favored candidate for resistive Fault Current Limiters (FCLs) [3]–[5].

The main principle of HTS-FCL is to utilize the transition from the superconducting to the normal-conducting state by exceeding the critical current density of the superconductor. This transition is obtained by a succession of quench, i.e. an abrupt and localized loss of superconductivity. Hence, the FCL performance is dependent on the quench propagation which switches the whole superconducting material to the normal state and then limits the current flow with the increase of resistivity. As a result of low thermal diffusivity and inadequate energy

dissipation, a considerable heating of the superconductive film can occur within the FCL. In the worst case, the HTS could not retrieve his superconducting state after the fault. Under these circumstances all the nominal current passes through a much resistive material and the device finally burns out by a fast Joule heating.

In the recent past, several authors have proposed numerical magneto-thermal models to describe the behavior of CC-FCL [6]–[8]. Such simulations are of great interest to design efficient limiters since they allow having a better understanding of these devices, which are hard to design in a way that thermal stability is ensured over all conditions of operation. Nonetheless, numerical models proposed in the literature are usually not suitable for quick and simple calculations. Indeed, implementing home developed code or using typical finite element method (FEM) software is often time consuming and requires considerable resources.

In this paper, we present a magneto-thermal model implemented in *COMSOL Multiphysics*, a widely used FEM package, that is simple to use and provide us an easy way to share engineering with academics and industries.

## 2. Theoretical model

Our geometrical model is based on a commercial coated conductor available from Theva [9]. The former tape is constituted of four layers: a thick conductive substrate layer made of Hastelloy C276, which is usually electrically isolated from the HTS; a MgO buffer layer; a superconductive film made of DyBCO ( $\text{DyBa}_2\text{Cu}_3\text{O}_7$ ) and a silver stabilizer in electrical contact with the superconductor. In order to simulate the CC-FCL behavior, we used a 2D geometry (a conductor of infinite length) 20 times thicker than the real one. As depicted in Figure 1, we intentionally omitted the buffer layer, which does not influence importantly the electromagnetic and thermal

behavior of the tape, to reduce the computation time.

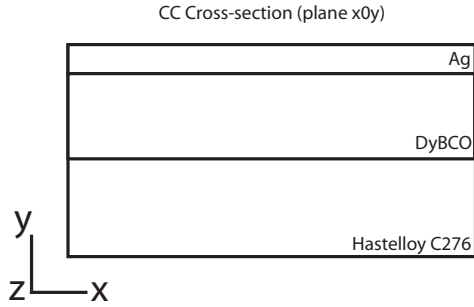


**Figure 1:** Cross section of the simulated CC (not drawn to scale). The tape is 10 mm wide and is composed of three layers: 1) Hastelloy substrate, 2) DyBCO film and 3) an Ag stabilizer. We intentionally omitted the MgO buffer layer to reduce the computation time of our simulations.

## 2.1 Multiphysics

Our 2D model was developed by coupling two set of equations representing the electrical and thermal behavior of the HTS [10]. The electromagnetic formulation is based on a direct used of the magnetic field as a state variable [1]. In summary, we used the COMSOL PDE general form with edge elements. The Ampère's law is also used as a boundary condition to impose a current trough all the 2D domains, then the flow of current passing within each subdomains is given by their resistivity as in simple parallel resistances. The magneto-thermal coupling in the HTS is achieved by means of the non-linear resistivity, which depends on the temperature and local current density. For the purpose of this work, we used a combined exponent power law for the HTS resistivity to illustrate our ability to introduce complex non-linear functions in our model. Accordingly, we used  $n=20$  for  $J < J_c$  and  $n=10$  for  $J \geq J_c$ .

$$\rho(J, T) = \begin{cases} \rho_{pl}(J, T) & , T < T_c \\ \rho_n & , T \geq T_c \mid \rho_{pl}(J, T) \geq \rho_n \end{cases} \quad (1)$$

$$\rho_{pl}(J, T) = \frac{E_0}{J_c(T)} \left( \frac{|J|}{J_c(T)} \right)^{n-1} \quad (2)$$

$$J_c(T) = J_{c0} \left( \frac{T_c - T}{T_c - T_0} \right)^\alpha, \quad T < T_c \quad (3)$$

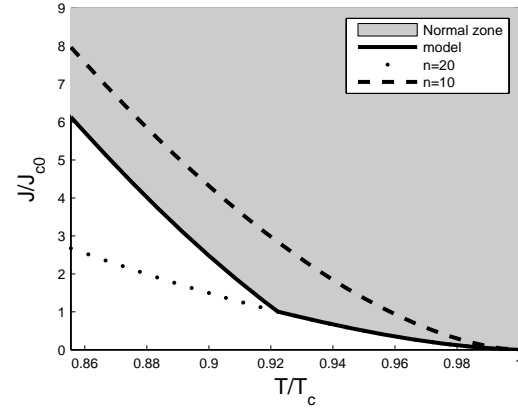


**Figure 2:** Normal resistivity frontier as a function of  $J$  and  $T$ . Our model is a combination of two power law i.e.  $n=10$  and  $n=20$ . The shaded area at the right of the curve represent the normal state (i.e  $\rho=130E-8\Omega.m$ ).

For the thermal part of our model, a common transient heat conduction equation was used.

$$\rho_m C_p \frac{\partial T}{\partial t} - \nabla \cdot (-k \nabla T) = E \cdot J \quad (4)$$

Where  $\rho_m$  is the resistivity,  $C_p$  the heat capacity,  $k$  the thermal conductivity tensor and  $E \cdot J$ , the Joule loss in the materials.

## 2.2 Heat transfer with a liquid nitrogen bath

A local increase of temperature in the HTS causes a reduction of the critical current which, in turn, changes the rotational of the magnetic field and the electric field inside the tape. This field generation is responsible of heat dissipation through the HTS that induces the loss of the superconducting state and may, ultimately, destroy the FCL. To avoid that, heat generated by Joule effect must be evacuated efficiently to keep the thermal stability of the device. This is done by means of conduction as well as thermal exchange with a liquid nitrogen bath. This last mechanism, called pool boiling, is mostly responsible of the heat transfer.

Due to the fact that pool boiling is dependent on the tape surface temperature, the system could become very unstable for a set of parameters that produce a film boiling regime –see Figure 3. In this case, the heat transfer is very low and the tape becomes almost thermally isolated.

With *COMSOL Multiphysics*, we used a convective heat flux at the interface between the

tape and liquid nitrogen. The boundary condition was set using the following equation.

$$q = h(T_s - T_0) \quad (5)$$

Where  $h$  is termed the convective heat transfer function of liquid nitrogen as represented on Figure 3.

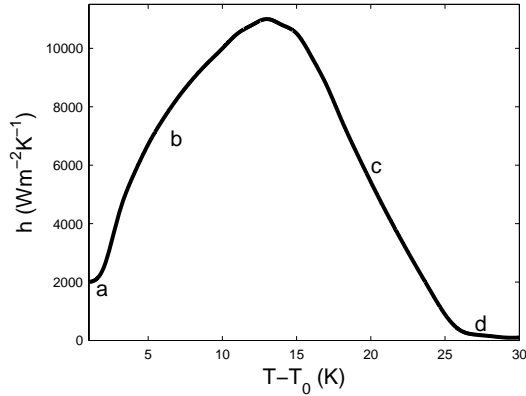


**Figure 3:** Convective heat transfer coefficient used for our model [11]. Usually, four regimes of heat transfer are observable with pool boiling a) free convection, b) nucleate boiling c) transition boiling and d) film boiling.

### 2.3 Numerical approximations

The simulations were developed in 2D for lower aspect ratio than the real FCL shape. This on account of the difficulty of meshing geometries of high aspect ratio that usually involves a large number of deformed elements. Following the work of Duron et al. [12], four physical parameters have been scaled in the thicker geometry to approximate the real solution. These parameters are  $C_p$ ,  $J_{c0}$ ,  $k$  and  $E$ .

Succinctly, the adopted numerical scheme is as follows. In all our simulations we kept the real total current in the hypertrophied tape, which is  $I$  time thicker than the real one. To do so, we divide  $J_{c0}$  by this  $I$  factor for the lower AR geometry. We also multiplied  $E$  by this factor to take into account the tape cross section (which is  $I$  time larger). For the thermal set of equations, the reduction of the  $y$  dimension has been implemented by a multiplication of  $k_y$  by  $I$ . A division of  $C_p$  by the  $I$  factor was also set to be consistent with the mass gain of the tape. Finally, we divide  $k_x$  by  $I$ , whereby to preserve the thermal diffusivity on the  $x$  direction.

Using lower AR geometries allows us to reduce the number of elements required to keep the convergence and accuracy of our model: with a reduced number of nodes, the shape of the elements and, consequently, the quality of the interpolated results can be improved. Figure 4 illustrates the influence of the problem size on the computation time. From this figure we can observe that the calculation time increase roughly as  $n_e=2.2$ . These times are those obtained on a dual Xeon quadcore E5355 with a 2.66GHz clock speed and 8GB of RAM memory. In our case using an AR 20 times larger allows reducing the number of elements from 19346 to 2516, which corresponds to a reduction of the computation time by 45.

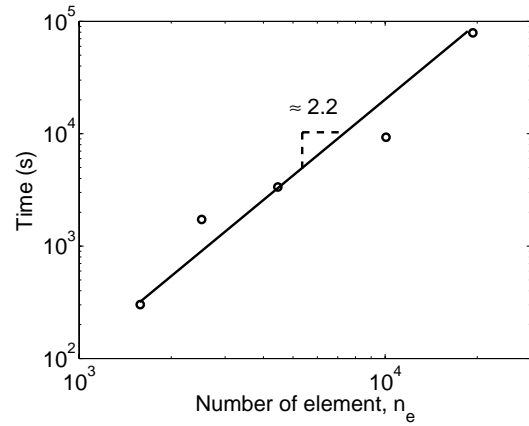
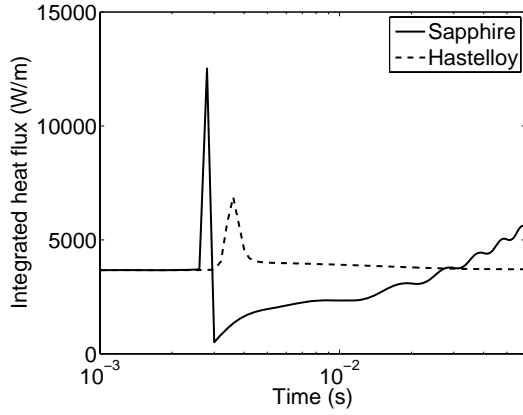


**Figure 4:** Computation time as a function of the number of element ( $n_e$ ). The dashed lines represent the slope of the curve.

### 3. A typical result

The materials constituting the tape have an important influence on the thermal exchange between the coolant and the tape surface. As depicted in Figure 9, by comparing two usual CC substrates, such as hastelloy and sapphire, we observe that a rapid increase of the surface temperature induce a huge drop on the thermal flux within the tape-coolant interface. The combination of a low heat capacity and a high thermal conductivity gives sapphire a thermal diffusivity (defined as  $\alpha = k/mC_p$ ) that is more than 1000 times larger than hastelloy. However, the heat, which is not readily stored in the sapphire substrate (low  $C_p$ ), can not be released due to the rapid increase of the surface temperature that led to the boiling regime

(Figure 3, region d). In this particular case, the heat transfer with the liquid nitrogen is at its minimum and led to quasi-adiabatic conditions.



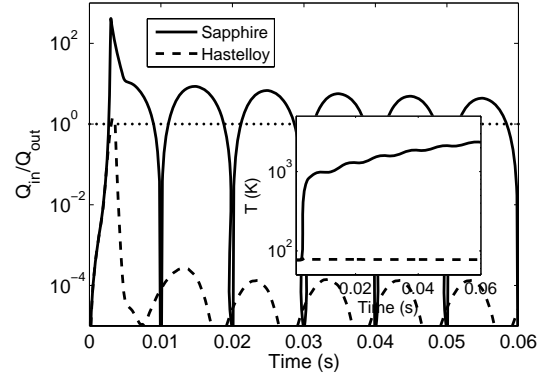
**Figure 5:** The integrated heat flux, which is defined as  $\oint h(T_s - T_0) dl$ , represent the heat exchange between the tape and the coolant. On the figure, we observe that the surface temperature of the sapphire substrate increase rapidly and make suddenly the convective coefficient reaching the film boiling region (the observed drop). At this stage, the tape is almost “isolated” from the coolant and it burn out quickly.

Figure 6 allows us to observe the stability criteria for these two cases (i.e. hastelloy and sapphire substrate). Stability recovery occurs when the heat removed to the substrate and coolant ( $Q_{out}$ ) is greater than that generated within the superconductor ( $Q_{in}$ ). The dot line plotted in Figure 6 is the graphical illustration of this criterion which is defined as:

$$\frac{Q_{in}}{Q_{out}} = \frac{\left[ \int_A \vec{E} \cdot \vec{J} dA' \right]_{HTS} + \left[ \int_A \vec{E} \cdot \vec{J} dA' \right]_{Ag}}{\oint h(T_s - T_0) dl} \quad (6)$$

We can see that sample made of sapphire have a notable energy gain at each half-cycle which also produce the continuous increase of the temperature (see inset of the figure 6). For this particular case, we can observe that the tape burned out almost instantaneously at the first current peak. The hastelloy curve let us observe that the denominator of equation 6, which is the liquid nitrogen exchange term, rapidly gets higher than the heat generation term (numerator). This leads to a fast thermal equilibrium with the surrounding coolant. Moreover, we observe in this figure that a “phase shift” exist between the produced energy within the hastelloy made tape and the imposed current to the device. This

comes from the flux diffusion phenomenon in the superconducting state, in which losses continue to occur within the sample through magnetic relaxation even if the source current is zero. In the case with sapphire, the temperature gets so high that superconductivity is rapidly lost, therefore no relaxation process exists.



**Figure 6:** Comparison of the heat balance for different substrate material. The heat generated in the tape made of sapphire is not evacuated at all. The temperature is continuously increasing until the device burned out. Inset is the temperature for both samples.

#### 4. Conclusions

In this paper we have presented a finite element model for studying electromagnetic and thermal behavior of HTS, specifically for FCL applications. The model is coupling the electromagnetic and thermal equations in a single solving process, is simpler to implement and much faster than other models based on solving the two parts separately and exchanging the results at each time step. The model, having been implemented in *COMSOL Multiphysics*, a widely used commercial software package (both in academic and industrial environment) and provides an easy way to share engineering knowledge between users.

#### 5. References

1. R. Brambilla, F. Grilli and L. Martini, Development of an edge-element model for AC loss computation of high-temperature superconductors, *Supercond. Sci. Technol.*, **20**, 16-24, (2007).
2. COMSOL Multiphysics documentation, AC/DC Module Model Library,

*Superconducting wire*, pp. 217-224. COMSOL Multiphysics (August 2006).

3. W. Prusseit, G. Sigl, R Nemetschek, C. Hoffman, J. Handke, A. Lümke and H. Kinder, Commercial coated conductor for fabrication based on inclined substrate deposition, presented at ASC 2004, Jacksonville, FL from Oct. 4-8, 2004, paper 1MR07 (2004).

4. Y. Li, J. Reeves, X. Xiong, Y. Qiao, Y. Xie, P.Hou, A. Knoll, K. Lenseth, and V. Selvamanickam, Fast growth process of long-length YBCO coated conductor with high critical current density, *IEEE Trans. Appl. Supercond.*, **15**, no. 2, 2771–2774 (2005).

5. M. Ahn, D. Bae, S. Yang, D. Park, T. Ko, C. Lee, B. Seok, and H. Chang, Manufacture and test of small-scale superconducting fault current limiter by using the bifilar winding of coated conductor, *IEEE Trans. Appl. Supercond.*, **16**, no. 2, 646–649 (2006).

6. M. Lindmayer and H. Mosebach, Quenching of high -  $T_c$  - superconductors and current limitation - numerical simulations and experiments, *IEEE Trans. Appl. Supercond.*, **7**, no. 2, 1029–1032 (1997).

7. T. Rettelbach and G. J. Schmitz, 3D simulation of temperature, electric field and current density evolution in superconducting components, *Supercond. Sci. Technol.*, **16**, 645–653 (2003).

8. J. Duron, F. Grilli, L. Antognazza, M. Decroux, B. Dutoit, and Ø. Fischer, Finite-element modelling of YBCO fault current limiter with temperature dependent parameters, *Supercond. Sci. Technol.*, **20**, no. 4, 338–344 (2007).

9. THEVA, Theva website, [www.theva.com](http://www.theva.com) (2007).

10. F. Roy, B. Dutoit, F. Grilli and F. Sirois, Magneto-Thermal Modeling of 2nd Generation HTS for Resistive Fault Current Limiter Design Purposes, Submitted to *IEEE Trans. Appl. Supercond.* (2007).

11. W. Frost and W. Harper, *Heat transfer at low temperatures*. Plenum press, 1975, ch. 4.

12. J. Duron, L. Antognazza, M. Decroux, F. Grilli, S. Stavrev, B. Dutoit, and Ø. Fischer, 3-D finite element simulations of strip lines in a YBCO/Au fault current limiter, *IEEE Trans. Appl. Supercond.*, **15**, no. 2, 1998–2002 (2005).

## 6. Acknowledgements

This work was partly supported by the Swiss National Science Foundation through the National Center of Competence in Research “Materials with Novel Electronic Properties - MaNEP” and partly by the US DOE Office of Electricity Delivery and Energy Reliability.